Generalized Poisson-Fermi formalism for investigating size correlation effects with multiple ions

Guillaume Tresset*
Institute of Bioengineering and Nanotechnology, 31 Biopolis Way, The Nanos 04-01, Singapore 138669
(Received 26 August 2008; revised manuscript received 21 November 2008; published 30 December 2008)

We establish a generalized Poisson-Fermi formalism to compute the electrostatic potential next to charged surfaces in the presence of multiple ion species with different sizes. A generalized Fermi-like ion distribution is deduced from the excess free energy, after expansion of the functional entropy of free space in which the ions have all the same size. The ion distribution is expressed in terms of the bulk volume fractions of each ion species rather than their bulk concentrations so as to account for the excluded volumes. We present size correlations effects such as underscreening and ion stratification, which have not been investigated before with such a simple theory. The change of dielectric properties across the space, arising from the finite spatial occupancy of ions, can be solved self-consistently through the Bruggeman model. The generalized Poisson-Fermi formalism is anticipated to be useful for interpreting electrophoretic mobility measurements and for computing the electrostatic potential over the surface of biomolecules in ionic solutions.

DOI: 10.1103/PhysRevE.78.061506 PACS number(s): 61.20.Qg, 82.60.Lf

I. INTRODUCTION

The electrostatic interactions between charged objects in solution and their ion atmosphere play an important role in biological processes and colloidal stability [1,2]. The folding of proteins and their biological activity [3–5], the compaction of genetic materials [6–11], the adsorption of ions onto lipid membranes [12–14], or the self-assembly of biomolecules [15–18] are amongst the numerous examples in biology where a theoretical description of the electrostatic interactions can lead to an improved understanding of the molecular functions in cells and to a better efficacy of drugs for biomedical applications.

The Poisson-Boltzmann theory [1,2] has been used for nearly one century to compute the distribution of ions surrounding charged surfaces. This theory considers pointlike ions interacting via their mean field in a continuum dielectric medium. The Poisson-Boltzmann theory has been useful to interpret a variety of experimental data on the binding of Mg^{2+} to nucleic acids [19,20]. It has also shown a fair agreement with the spatial distribution of small monovalent ions near a charged monolayer and inferred from resonant x-ray reflectivity measurements in salt-free conditions [21]. More comprehensive models based on integral equation theories [22,23] or Monte Carlo simulations have shown several discrepancies with the classical Poisson-Boltzmann approach due to correlation effects arising from the size of ions [24–27] and from the spatial fluctuations of the electrostatic potential [28–32]. These models have pointed out the importance of different sizes in the ion-ion interaction for monovalent systems [33]. The composition of the electrical double layer can be altered compared to the classical theory because the increase of the effective excluded volume of ions results in a decrease of the system bulk entropy that favors the tendency of ions to be adsorbed; it can thus lead to a surface overcharging where an apparent charge is adsorbed onto a like-charged wall [34]. Experimental investigations have also revealed a stratification of ions in the vicinity of a charged surface, attributed among other things, to the close packing of macroions [35]. The importance of ion sizes and ion-solvent interactions in the ion distributions has been also evidenced through x-ray reflectivity measurements of the interface between two electrolyte solutions; the Poisson-Boltzmann theory could not fully reproduce the experimental data without the use of a potential of mean force obtained separately by molecular dynamic simulations [36].

Integral equation theories and particle simulations, however, lack the simple physical picture provided by a Poisson-Boltzmann type of approach. An integrated theory accounting for the above mentioned effects would be of great importance for the mathematical modeling of phenomena taking place in ionic solutions [37–39]. The problem of volume exclusion in many-body systems dates back to the van der Waals description of real gas which finds a statistical mechanic justification through the lattice gas model [40]. The lattice model has been successfully used to account for the excluded-volume interaction of various systems in soft matter physics: it allows the computation of the Flory-Huggins free energy of polymer chains [41] or it predicts the phase separation of binary mixtures of colloids [42]. Likewise, the lattice model was applied to ionic systems of monodisperse size distribution [43–45], that is, for which ions have all the same size, and it predicted the formation of a saturated layer near a highly charged wall as a result of the close packing of the counterions [44,45]. The ions obeyed a Fermi-like distribution and consequently the electrostatic potential was rather given by a Poisson-Fermi equation. More sophisticated techniques rely on density functional theory to compute the excess free energy [46–50] which, thanks to a weighted-density approximation, can correct the Poisson-Boltzmann theory in accord with Monte Carlo simulations [51]. Such theories are accurate for monodisperse hard sphere liquids but they introduce an additional degree of complexity in their treatment, and pose a number of computational challenges when applied to biomolecules with tortuous topology. The question of polydisperse systems—where different ion species with different sizes are considered—although ubiquitous in biology, has been scarcely addressed

*Present address: Laboratoire de Physique des Solides, Université Paris-Sud, CNRS, UMR 8502, F-91405 Orsay Cedex, France. tresset@lps.u-psud.fr

so far with a Poisson-Boltzmann-like approach. The ion-size asymmetry can be accounted for by allocating a heuristic dependence on the electrostatic potential to the ion volume fraction [37]. In a less empirical manner, Chu and coworkers assessed the binding properties of ions to DNA duplexes using a size-modified Poisson-Boltzmann theory [52]. Considering two populations of ions only, they used the lattice model to solve the electrostatic potential next to a DNA rod, and arrived at a good agreement with experimental data by adjusting the ion-size parameters.

In the present work, we introduce a generalized Poisson-Fermi formalism applicable to polydisperse systems of multiple ions. The distributions of ions are hence described in terms of bulk volume fractions of each ion species rather than just their bulk concentrations. An arbitrary number of excluded volumes can be taken into account in contrast to the previously mentioned work by Chu and co-workers [52]. Size correlation effects, which have not been studied before in the framework of such a simple theory, are exemplified next to a charged wall: underscreening, saturated layer of mixed ions and ion stratification are reported. At last, we propose a self-consistent way to compute the change of the effective dielectric constant as the ion volume fractions vary across the solution.

II. DETERMINATION OF THE FREE ENERGY AND ION DISTRIBUTIONS

A. Lattice gas model for monodisperse systems

To begin, we consider a solution containing M ion species of valence $z_i (1 \leqslant i \leqslant M)$, and volume fraction $\phi_i \equiv c_i v_i$, where c_i is the concentration and v_i the excluded volume. The volume fractions always verify $0 \leqslant \phi_i \leqslant 1$. Note that the solvent can be readily included as an ion species of valence zero. There is no general expression for the free energy of such a system, so we need to proceed first by considering the monodisperse situation where all the ions have an identical excluded volume $v_1 = \cdots = v_M \equiv v$. We use a lattice gas model [40,53] in which the ions are placed in discrete cells of volume v, and we will later extend the free energy to the polydisperse situation. The ion species occupies each $N_1 \cdots N_M$ sites of the lattice in such a way that no two ions occupy the same site. The total number of ions is $N \equiv N_1 + \cdots + N_M$ distributed across the lattice of volume V made of R sites so that $V = Rv$. Quite generally, the canonical partition function in phase space $(\mathbf{r}^N, \mathbf{p}^N)$ is

$$Z(\beta, V, N_1, \ldots, N_M; v) = \frac{1}{N_1!} \cdots \frac{1}{N_M!} \frac{1}{h^{3N}} \int d\mathbf{r}^N \int d\mathbf{p}^N \exp[-\beta \mathcal{H}(\mathbf{r}^N, \mathbf{p}^N)], \tag{1}$$

where $\beta \equiv 1/k_B T$ with k_B the Boltzmann constant and T the temperature, and h is the Planck constant. The Hamiltonian $\mathcal{H}$ can be written as

$$\mathcal{H}(\mathbf{r}^N, \mathbf{p}^N) = \sum_{k=1}^{N} \frac{p_k^2}{2m_k} + \sum_{k=1}^{N} z_k e \psi(\mathbf{r}_k) + \sum_{k \neq l} U(\mathbf{r}_k, \mathbf{r}_l), \tag{2}$$

with m_k the mass of particle k, $\psi(\mathbf{r}_k)$ the electrostatic potential, and $U(\mathbf{r}_k, \mathbf{r}_l)$ the potential of hardcore repulsion between two particles k and l. The latter potential is $+\infty$ when two ions occupy the same site, that is, $|\mathbf{r}_k - \mathbf{r}_l| \leqslant d$ with d the distance separating the lattice cells ($v \equiv d^3$), and zero otherwise. The term arising from the kinetic energy in the Hamiltonian can be integrated over the whole range of momenta $\mathbf{p}$. A usual simplification for the electrostatic energy is to consider that the ions interact with one another through their mean field potential ψ, constant over the volume V in consideration. The canonical partition function now reads

$$Z(\beta, V, N_1, \ldots, N_M; v) = \frac{1}{N_1!} \cdots \frac{1}{N_M!} \frac{1}{\Lambda_1^{3N_1}} \cdots \frac{1}{\Lambda_M^{3N_M}} \exp\left(-\beta \sum_{i=1}^{M} z_i e N_i \psi \right) \times \int d\mathbf{r}^N \exp\left[-\beta \sum_{k \neq l} U(\mathbf{r}_k, \mathbf{r}_l) \right], \tag{3}$$

where $\Lambda_i = h/(2\pi m_i k_B T)^{1/2}$ is the de Broglie thermal wavelength of ion species i. The integral can be evaluated by placing the N indistinguishable ions on R lattice sites with no two ions occupying the same site. It yields

$$\int d\mathbf{r}^N \exp\left[-\beta \sum_{k \neq l} U(\mathbf{r}_k, \mathbf{r}_l) \right] = Rv \cdots (R - N + 1)v = v^N \frac{R!}{(R-N)!}. \tag{4}$$

The free energy is then

$$F(\beta, V, N_1, \ldots, N_M; v) = -k_B T \ln[Z(\beta, V, N_1 \ldots N_M; v)] = \sum_{i=1}^{M} z_i e N_i \psi + k_B T \sum_{i=1}^{M} N_i \ln\left(\frac{N_i}{R} \frac{\Lambda_i^3}{v} \right) + k_B T R \left(1 - \sum_{i=1}^{M} \frac{N_i}{R} \right) \ln\left(1 - \sum_{i=1}^{M} \frac{N_i}{R} \right), \tag{5}$$

where we have used the Stirling's approximation $\ln X! \approx X \ln X - X$ for large X.

B. Extension to polydisperse systems

The density of free energy in the thermodynamic limit $f \equiv F/V$ can be obtained from Eq. (5) by noticing that the ion concentrations are $c_i = N_i/Rv$. The free energy is then rewritten as a functional of the ion concentrations by integrating f over a domain Ω of the space $F = \int_\Omega f d\mathbf{r}$, and can be decomposed into an ideal Coulomb gas free energy F_{id} and an excess free energy F_{ex} such that

$$F(\beta, c_1, \ldots, c_M; v) \equiv F_{\mathrm{id}} + F_{\mathrm{ex}}, \tag{6}$$

with

$$F_{\mathrm{id}}(\beta,c_1,\ldots,c_M;v) \equiv \int_\Omega \left\{ \sum_{i=1}^{M} z_i e c_i \psi + k_B T \sum_{i=1}^{M} c_i \ln(c_i \Lambda_i^3) \right\} d\mathbf{r} \quad (7)$$

and

$$F_{\mathrm{ex}}(\beta,c_1 \ldots c_M;v) \equiv TS_{\mathrm{FS}}(c_1 \ldots c_M;v) \equiv T\int_\Omega k_B \frac{1}{v} \phi_{\mathrm{FS}}(v) \ln \phi_{\mathrm{FS}}(v) d\mathbf{r}. \quad (8)$$

We define here $\phi_{\mathrm{FS}}(v) \equiv 1 - c_1 v - \cdots - c_M v$ the volume fraction of free space for a monodisperse system. S_{FS} stands for the entropy of free space. It reduces the total entropic contribution in the free energy as the ions lose spatial freedom due to their volume exclusion. Note that the ideal Coulomb gas free energy F_{id} generally includes an additional term under the integral, proportional to the ion concentrations, $-k_B T \Sigma c_i$ [23]. This term is here cancelled by an opposite contribution arising from the excess free energy and is therefore omitted for clarity. The volume fraction of free space for a polydisperse system is

$$\phi_{\mathrm{FS}}(v_1,\ldots,v_M) \equiv 1 - \phi_1 - \cdots - \phi_M. \quad (9)$$

In order to express S_{FS} in the polydisperse case, we carry out an expansion in Taylor series of $S_{\mathrm{FS}}(c_1,\ldots,c_M;v_1,\ldots,v_M)$ close to an excluded volume of reference v_{ref}. To this end, we actually expand $(S_{\mathrm{FS}} - \int_\Omega k_B \vartheta^{-1} \phi_{\mathrm{FS}} \ln \phi_{\mathrm{FS}} d\mathbf{r})$ given as a function of $v_1,\ldots,v_M$ and where $\vartheta(v_1,\ldots,v_M)$ is an effective excluded volume for the system, verifying the following properties:

$$\forall (v_1,\ldots,v_M) \begin{cases} k_B \vartheta^{-1} \phi_{\mathrm{FS}} \ln \phi_{\mathrm{FS}} \text{ is } C^\infty, \\ \min_i v_i \leqslant \vartheta(v_1,\ldots,v_M) \leqslant \max_i v_i. \end{cases} \quad (10)$$

In particular, we see immediately that $\forall v\, \vartheta(v) = v$. The expansion thereby yields

$$S_{\mathrm{FS}}(c_1,\ldots,c_M;v_1,\ldots,v_M) = \int_\Omega k_B \vartheta^{-1} \phi_{\mathrm{FS}} \ln \phi_{\mathrm{FS}} d\mathbf{r} + \sum_{i=1}^{M} \varepsilon_{v,i} \int_\Omega \Delta \mathsf{S}_i \, d\mathbf{r} + o(\max_i |\varepsilon_{v,i}|), \quad (11)$$

where $\varepsilon_{v,i} \equiv (v_i - v_{\mathrm{ref}})/v_{\mathrm{ref}}$ and the functional coefficients of the series verify

$$\int_\Omega \Delta \mathsf{S}_i(c_1,\ldots,c_M;v_{\mathrm{ref}}) d\mathbf{r} \equiv v_{\mathrm{ref}} \frac{\partial}{\partial v_i} \left(S_{\mathrm{FS}} - \int_\Omega k_B \vartheta^{-1} \phi_{\mathrm{FS}} \ln \phi_{\mathrm{FS}} d\mathbf{r} \right) \Bigg|_{v_{\mathrm{ref}}}. \quad (12)$$

The properties of the effective excluded volume ϑ in Eq. (10) allow us to recover the entropy of free space in the monodisperse case (8) from the expansion (11) for any excluded volume v, provided that the sum of the functional coefficients of the expansion also verify $\forall (c_1,\ldots,c_M;v_{\mathrm{ref}}) \Delta \mathsf{S}_1 + \cdots + \Delta \mathsf{S}_M = 0$. A possible way to evaluate these functional coefficients might be to identify them with correlation functions known from integral equation theories such as the mean spherical approximation [23].

We can hence write the free energy of a polydisperse system occupying a region Ω of the space, coupled to a reservoir of ions through the chemical potentials μ_i and immersed in a medium of dielectric constant ε:

$$F(\beta,\psi,c_1,\ldots,c_M;v_1,\ldots,v_M) = \int_\Omega \left\{ -\frac{|\nabla\psi|^2}{2\varepsilon\varepsilon_0} + \sum_{i=1}^{M} z_i e c_i \psi + k_B T \sum_{i=1}^{M} c_i \ln(c_i \Lambda_i^3) - \sum_{i=1}^{M} \mu_i c_i + k_B T \vartheta^{-1} \phi_{\mathrm{FS}} \ln \phi_{\mathrm{FS}} \right\} d\mathbf{r} + \sum_{i=1}^{M} \varepsilon_{v,i} T \int_\Omega \Delta \mathsf{S}_i \, d\mathbf{r} + o(\max_i |\varepsilon_{v,i}|), \quad (13)$$

where ε_0 is the permittivity of free space. The chemical potentials μ_i are obtained by minimization of Eq. (13) with respect to concentrations c_i for any domain Ω,

$$\mu_i(\beta,\psi,c_1,\ldots,c_M;v_1,\ldots,v_M) = [z_i e \psi + k_B T \ln(c_i \Lambda_i^3) - k_B T \ln \phi_{\mathrm{FS}}] + \left\{ (\varepsilon_\vartheta - \varepsilon_{v,i}) k_B T [1 + \ln \phi_{\mathrm{FS}}] + \sum_{j=1}^{M} \varepsilon_{v,j} T \frac{\partial \Delta \mathsf{S}_j}{\partial c_i} \right\} + o(\max_j |\varepsilon_{v,j}|). \quad (14)$$

ε_ϑ is defined by $\varepsilon_\vartheta \equiv (\vartheta - v_{\mathrm{ref}})/v_{\mathrm{ref}}$ and we know from Eq. (10) that $\min_i \varepsilon_{v,i} \leqslant \varepsilon_\vartheta \leqslant \max_i \varepsilon_{v,i}$. Assuming the excluded volumes are dispersed from each other up to a reasonable extent, the chemical potentials can be reduced to their zeroth-order term, that is,

$$\mu_i(\beta,\psi,c_1,\ldots,c_M;v_1,\ldots,v_M) \approx z_i e \psi + k_B T \ln(c_i \Lambda_i^3) - k_B T \ln \phi_{\mathrm{FS}}(v_1,\ldots,v_M). \quad (15)$$

Notice that this form of approximated chemical potential does not allow by itself the existence of the free energy functional because it does not define an exact differential in the polydisperse case $\partial \mu_i / \partial c_j \neq \partial \mu_j / \partial c_i$ for $i \neq j$.

C. Generalized Fermi-like distribution with polydisperse volume exclusion

At thermodynamical equilibrium, the chemical potentials of each ion species must be constant across the space, that is,

$$\mu_i(\beta,\psi,c_1,\ldots,c_M;v_1,\ldots,v_M) = \mu_i(\beta,0,c_1^\infty,\ldots,c_M^\infty;v_1,\ldots,v_M), \quad (16)$$

where the superscript ∞ denotes quantities evaluated in the reservoir, namely, at infinity, where the electrostatic potential

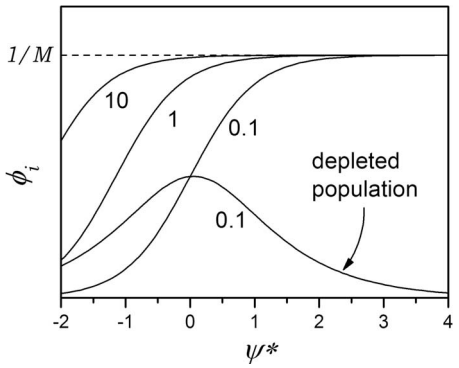

FIG. 1. Generalized Fermi-like distribution of a system with multiple ions. The volume fraction ϕ_i versus the dimensionless electrostatic potential is calculated according to Eq. (19). M (=10 in this example) ion species of valence −2 are considered with an identical ratio $\phi_i/\phi_{\mathrm{FS}}^{\infty}$ for every species. The figures next to the curves indicate the value of $\phi_i/\phi_{\mathrm{FS}}^{\infty}$. The curve of depleted population is the distribution of an ion species of valence −1, all the others being of valence −2.

is set to zero. The temperature is maintained constant as usual for biological solutions. Using the approximated chemical potential of Eq. (15), Eq. (16) can be rearranged into a relation between the volume fractions and the dimensionless electrostatic potential $\psi^* \equiv e\psi/k_BT$ only:

$$\phi_1 + \phi_2 + \cdots + \left[1 + \frac{\phi_{\mathrm{FS}}^{\infty}}{\phi_i^{\infty}} \exp(z_i\psi^*)\right]\phi_i + \cdots + \phi_M = 1,$$

$$1 \leqslant i \leqslant M. \tag{17}$$

We have therefore a system of M equations with $M+1$ unknown. Subtracting equalities (17) written for two distinct ion species i and j yields a relation between the volume fractions ϕ_i and ϕ_j in any point of the space, the bulk quantities being fixed:

$$\frac{\phi_i}{\phi_i^{\infty}} = \frac{\phi_j}{\phi_j^{\infty}} \exp[(z_j - z_i)\psi^*]. \tag{18}$$

Injecting the relations (18) for every $j \neq i$ into Eq. (17) written for a chosen i gives us the distribution of volume fraction for each ion species

$$\phi_i = \frac{\exp(-z_i\psi^*)\phi_i^{\infty}}{\phi_{\mathrm{FS}}^{\infty} + \Sigma_{j=1}^{M} \exp(-z_j\psi^*)\phi_j^{\infty}}, \quad 1 \leqslant i \leqslant M. \tag{19}$$

Equation (19) is the counterpart of the Boltzmann distribution in the classical theory with pointlike particles. This relation is reminiscent to the Fermi distribution as it reflects the lattice-saturation effect for which the system cannot exceed the allowed maximum of ion concentration whatever its polarization [37]. A further refined formula along with a possible expression for the effective excluded volume is presented in the Appendix. Figure 1 illustrates the form of this generalized Fermi-like distribution for given valences and volume fractions in the bulk. The saturation effect is clearly visible at high electrostatic potential. However, the saturation may not take place, leading instead to a depletion of a specific ion population. The volume fraction $\phi_i(\psi^*)$ of ion population i with valence z_i peaks when

$$\sum_{j=1}^{M} (z_j - z_i)\exp(-z_j\psi^*)\frac{\phi_j^{\infty}}{\phi_{\mathrm{FS}}^{\infty}} = z_i, \tag{20}$$

which means that there must be an ion species j of valence z_j such that $\mathrm{sgn}(z_j)=\mathrm{sgn}(z_i)$ and $|z_j|>|z_i|$. The ion species i will then be depleted at the benefit of the species j.

The minimum free energy F_{min} of the system is given by injecting the generalized Fermi-like distribution (19) into the general equation (13). It reads

$$F_{\mathrm{min}}(\beta, \psi^*, c_1^{\infty}, \ldots, c_M^{\infty}; v_1, \ldots, v_M) \approx \int_{\Omega} \left\{ -\frac{|\nabla\psi|^2}{2\varepsilon\varepsilon_0} - k_BT\vartheta^{-1} \times \ln\left[1 + \sum_{i=1}^{M} \exp(-z_i\psi^*)\frac{\phi_i^{\infty}}{\phi_{\mathrm{FS}}^{\infty}}\right]\right\} d\mathbf{r}. \tag{21}$$

Interestingly, the knowledge of ϑ is not needed in the generalized Fermi-like distribution (19) but is required for computing the minimum free energy of the system.

III. SIZE CORRELATION EFFECTS WITH POLYDISPERSE IONS NEAR A CHARGED WALL

A. Saturated layer and underscreening

The electrostatic potential is related to the charge density by the Poisson equation that reads

$$\nabla(\varepsilon\varepsilon_0 \nabla \psi^*) = -\beta e^2 \sum_{i=1}^{M} z_i c_i. \tag{22}$$

The combination of Eqs. (19) and (22) shall be called hereafter the generalized Poisson-Fermi equation and will allow us to consistently compute the electrostatic potential and the ion volume fractions across the space. Notice that at low electrostatic potentials $\psi^* \ll 1$, and homogeneous dielectric medium, the Debye-Hückel approximation is recovered, and the inverse Debye length keeps its usual form $\kappa = [(\beta e^2/\varepsilon\varepsilon_0)\Sigma c_i^{\infty} z_i^2]^{1/2}$. In the present study, we will limit ourselves to the electrostatic potential and the ion distributions next to a wall of charge density $\sigma_0 < 0$ occupying the plane $x=0$. All the quantities are thereby function of x only, and the differential operator in Eq. (22) is reduced to $d_x(\varepsilon\varepsilon_0 d_x\psi^*)$ with the notation $d_x = d/dx$. The boundary conditions for ψ^* are then $d_x\psi^*(x=0) = -\beta e\sigma_0/\varepsilon\varepsilon_0$ and, as before, $\psi^*(x \to +\infty) = 0$. The Poisson-Fermi equation verifying the boundary conditions was solved numerically by a collocation method implemented under MATLAB™. The infinity was fixed at tenfold the Debye length κ^{-1} from the wall.

In view of using our theory for ionic titration by electrophoretic mobility [12,16], we consider a bulk solution made of 10 mM of a 1:1 electrolyte referred to as the buffer electrolyte, and of a 1:1 electrolyte with a variable concentration c^{∞} referred to as the added electrolyte. The added ions have an excluded volume of 0.8 nm^3 while the buffer ions have a

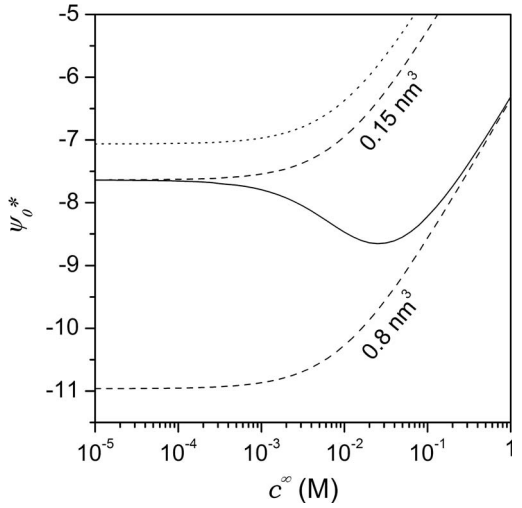

FIG. 2. Comparison between monodisperse and polydisperse situations through the dimensionless surface potential ψ_0^* of a charged wall as a function of the concentration of added ions c^∞. The solution is made of 10 mM of a 1:1 buffer electrolyte and a 1:1 added electrolyte. The wall has a surface charge density of $\sigma_0 = -0.2$ C m^{-2}. The solid line is the numerical solution from the generalized Poisson-Fermi equation with an excluded volume for added ions of 0.8 nm^3, and for buffer ions fixed at 0.15 nm^3. The dashed lines represent the numerical solutions for the Poisson-Fermi equation where all ions have an identical excluded volume indicated next to the curves. The dotted line arises from the classical Poisson-Boltzmann theory.

fixed excluded volume of 0.15 nm^3. Figure 2 shows the result obtained from the generalized Poisson-Fermi equation with a polydisperse population of ions (solid line). This numerical solution connects nicely those obtained with monodisperse populations (dashed lines) with 0.15 and 0.8 nm^3 of excluded volume, which are predominant at low and high concentrations of added ions, respectively. The Poisson-Boltzmann theory (dotted line) expectedly yields a large discrepancy.

Figure 3(a) shows the dimensionless surface potential of the wall ψ_0^* versus c^∞ and the excluded volume of added counterions v. At high v, we see that ψ_0^* transiently drops as if the wall became more negatively charged. As c^∞ increases, the screening effect comes into play and ψ_0^* tends again to neutrality so that the function $\psi_0^*(c^\infty)$ exhibits a minimum. We have plotted in Fig. 3(b) the dimensionless surface potential ψ_0^* normalized to its value obtained from the Poisson-Boltzmann theory in order to remove the contribution from the pointlike screening effect. The wall seems thereby to be underscreened in the sense that size correlations give rise to less screening than what is predicted by the Poisson-Boltzmann theory alone for the same ionic bulk concentrations. Such a drop in the surface potential has been reported before with the electrophoretic mobility of latex nanoparticles in the presence of divalent cations, and confirmed by simulations based on integral equations theory [25].

What gives rise to this underscreening? Figure 4 shows the normalized volume fractions across the solution at the concentration of added ions that makes ψ_0^* minimal in Fig.

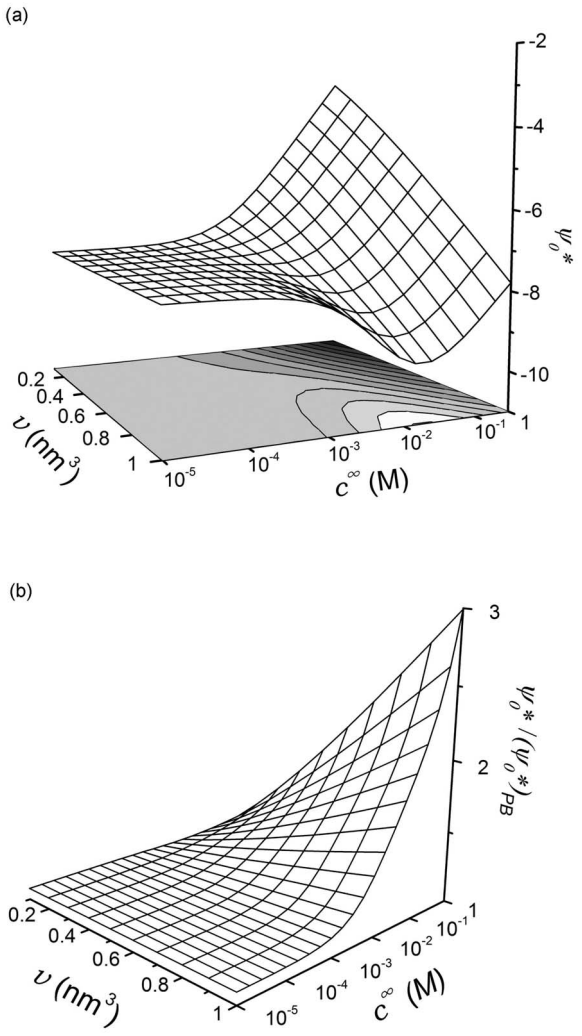

FIG. 3. (a) Dimensionless surface potential ψ_0^* of a charged wall as a function of the concentration of added ions c^∞ and of their excluded volume v. The solution and the charge of the wall are the same as in Fig. 2. (b) Dimensionless surface potential ψ_0^* normalized to its value given by the Poisson-Boltzmann theory $(\psi_0^*)_{PB}$ plotted versus c^∞ and v for the same conditions.

3(a). The counterions (+1) form a saturated layer near the wall in which their concentration approaches their close packing value. On the other hand, the coions (−1) are strongly depleted with respect to the classical theory. The fact that the counterions cannot exceed their close packing concentrations results in more negative electrostatic potentials (Fig. 4 inset) within the saturated layer compared to the classical theory: if we consider Eqs. (15) and (16) written for a counterion species inside the saturated layer ($\phi_{FS} \to 0$), the electrostatic contribution $z_i e\psi$ must balance the loss of entropy due to the saturation in order to equilibrate the chemical potential with its bulk value.

In Eq. (18), when ions i and j have the same valence, their normalized volume fractions are equal across the solution $\phi_i / \phi_i^\infty = \phi_j / \phi_j^\infty$. The profiles depicted in Fig. 4 thereby hold true both for the added and buffer ions. In the general case, let us assume z_{sat} be the valence of the ions forming a saturated layer. Since we are inside the saturated layer, we have

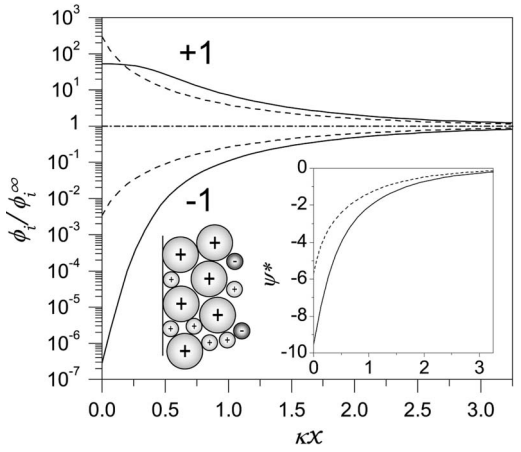

FIG. 4. Ion volume fractions normalized to their bulk value next to a charged wall. The concentration of added ions is $c^\infty=30$ mM, the excluded volume of added counterions $v=1$ nm^3, and the other parameters are the same as those in Fig. 2. The solid lines are solutions computed with the generalized Poisson-Fermi equation while the dotted lines are from the Poisson-Boltzmann theory. The labels +1 and −1 indicate the profiles of counterions and coions respectively. In inset, the profile of the dimensionless electrostatic potential is plotted for both theories.

$\Sigma_k \phi_k \approx 1$, where k refers to all the ion species of valence z_{sat}. As a consequence of the equality on the normalized volume fractions for ions of same valence, the charge density inside the saturated layer is constant: $\rho_{\text{sat}} \approx z_{\text{sat}} e \Sigma_k c_k^\infty / \Sigma_k \phi_k^\infty$ and the electrostatic potential given by the generalized Poisson-Fermi equation in a homogeneous dielectric medium becomes a quadratic function of the space coordinate.

B. Hierarchical stratification of multivalent ions

We now turn our attention to electrolytes with counterions of different valences. If we assume $z_i > z_j$ and the ions i form a saturated layer (high $z_i\psi^*$), then according to Eq. (18)—or equivalently Eq. (20)—the ions j will be strongly depleted. Resulting profiles are depicted in Fig. 5(a). In that case, the ions undergo a hierarchical stratification where successive layers enriched in ions of decreasing valence build up starting from the wall. The global saturated layer extends up to 1.5 times the Debye length, with saturated trivalent cations coming first, then a layer of divalent cations and around 50% of monovalent cations at the edge of the global saturated layer. This stratification of ions cannot be predicted by the Poisson-Boltzmann theory for which the cations are attracted onto the wall by the electrostatic force regardless their spatial occupancy [Fig. 5(b)].

Figure 6 compares the ion volume fractions for the same system when the excluded volumes of cations are 1 nm^3 for all of them (dashed lines) and when those of divalent and monovalent cations become 0.7 and 0.8 nm^3, respectively (solid lines). As expected, the layers become narrower with smaller excluded volumes. We see also that even the layer of unchanged trivalent cations is affected by the other cations because these latter can penetrate into the layer of trivalent cations more easily thanks to their smaller size. Furthermore,

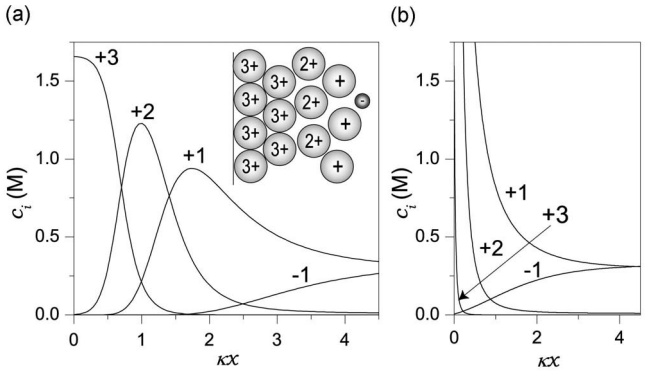

FIG. 5. Spatial repartitions of ions with different valences. The solution is made of three electrolytes: a 3:1 at 10 μM, a 2:1 at 10 mM, and a 1:1 at 300 mM. The wall has a charge density of $\sigma_0=-0.4$ C m^{-2}. All the counterions have an excluded volume of 1 nm^3 and the coions 0.15 nm^3. (a) Ion concentrations given by the generalized Poisson-Fermi equation. The inset is a schematic of the ion stratification next to the wall. (b) Ion concentrations given by the Poisson-Boltzmann theory. The numbers next to the curves on (a) and (b) indicate the ion valence.

the layers are not necessarily saturated (volume fractions significantly lower than 1) and we can find a lower bound for their maximal value $\phi_i^{\max}$. Inside a layer, the ion species i is dominant, and consequently $\phi_{\text{FS}} \approx 1 - \phi_i^{\max}$. The thermodynamic equilibrium condition on the chemical potential—Eqs. (15) and (16)—at the maximal volume fraction, then leads to

$$z_i \psi^* \approx \ln\left(\frac{1-\phi_i^{\max}}{\phi_i^{\max}} \frac{\phi_i^\infty}{\phi_{\text{FS}}^\infty} \right). \tag{23}$$

Since $z_i\psi^* < 0$ because we consider here counterions, we obtain the following inequality:

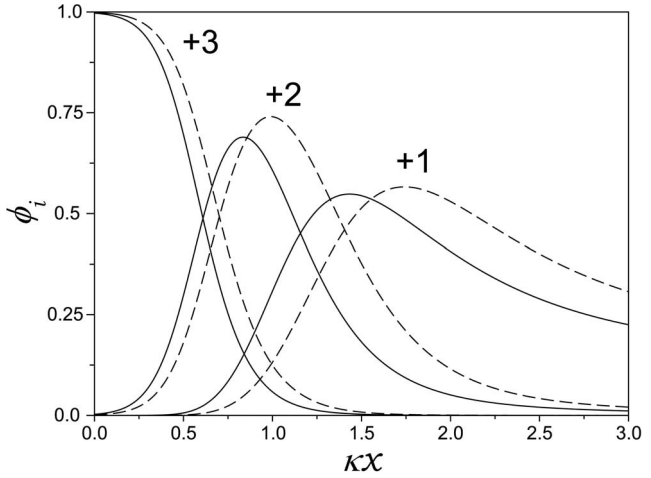

FIG. 6. Effect of the excluded volume on the ion stratification. The dashed lines represent the volume fractions of ions in the same conditions as in Fig. 5. The solid lines are the volume fractions when the excluded volumes become 0.7 and 0.8 nm^3 for divalent and monovalent cations respectively. Trivalent cations and anions keep an excluded volume of 1 and 0.15 nm^3, respectively. The numbers next to the curves indicate the ion valence.

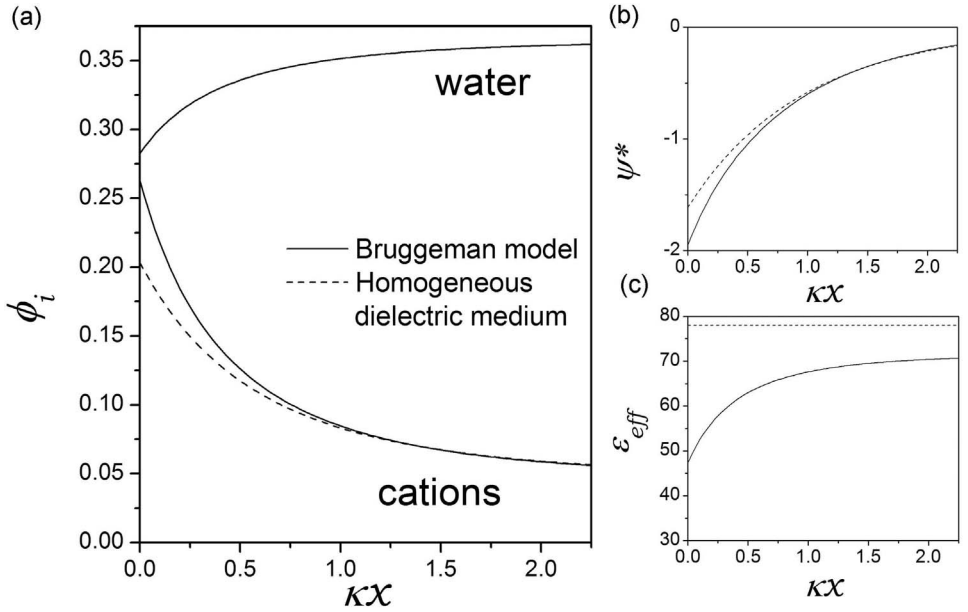

FIG. 7. Effects of the dielectric solvent (water) on the ion repartition. The solution is made of 80 mM of 1:1 added electrolyte with 10 mM of 1:1 buffer electrolyte. The excluded volume of added cations is 1 nm^3 while the rest of ions have an excluded volume of 0.15 nm^3. The surface charge density of the wall is only $\sigma_0=-0.03$ C m^{-2}. The water molecules have an excluded volume of 0.011 nm^3 (effective radius of ~1.4 Å) and a concentration of 55 M. The dielectric constants of free space and water molecules are 78 while the ions in solution have a dielectric constant of 1. The solid lines denote numerical solutions obtained with the Bruggeman model and the dashed lines label the solutions with a homogeneous medium of dielectric constant 78. (a) Volume fractions of added cations and water molecules. (b) Dimensionless surface potential. (c) Effective dielectric constant. The Debye length κ^{-1} is calculated with the dielectric constant of water, namely, 78.

$$\phi_i^{\max} > \frac{1}{1+\frac{\phi_i^\infty}{\phi_{\mathrm{FS}}^\infty}}. \tag{24}$$

Equation (24) tells us that counterion species occupying a small volume fraction in the bulk with respect to the free space (low $\phi_i^\infty/\phi_{\mathrm{FS}}^\infty$) will be prone to become packed in an enriched layer formed next to the wall.

The profiles in Figs. 5(a) and 6 must be considered carefully because the electrostatic correlation effects, which become important with multivalent ions, are not included into the generalized Poisson-Fermi equation. These effects tend to diminish the repulsion between like-charged ions so that the enriched layers are expected to build up for smaller electrostatic potentials.

C. Ionic repartition with dielectric solvent model

So far the solvent has been considered implicitly as a continuum of dielectric constant ε. We see from the generalized Fermi-like distribution (19) that introducing solvent particles of zero valence has no influence upon the volume fractions of ions, and their concentration does not even enter the Poisson equation (22). The solvent therefore only intervenes through the dielectric properties it confers to the system. As the counterions are attracted onto the wall and build up an enriched layer, the dielectric constant is no longer the same across the solution and depends on the local volume fractions of ion species. An effective dielectric constant $\varepsilon_{\mathrm{eff}}$ can be computed through the Bruggeman equation [54,55]

$$\sum_{i=1}^{M} \phi_i \frac{\varepsilon_i - \varepsilon_{\mathrm{eff}}}{\varepsilon_i + 2\varepsilon_{\mathrm{eff}}} + \phi_{\mathrm{FS}} \frac{\varepsilon_{\mathrm{FS}} - \varepsilon_{\mathrm{eff}}}{\varepsilon_{\mathrm{FS}} + 2\varepsilon_{\mathrm{eff}}} = 0, \tag{25}$$

where ε_i and $\varepsilon_{\mathrm{FS}}$ denote the dielectric constants of ion species i and of free space, respectively. The resulting effective dielectric constant must be substituted into the Poisson equation (22) but also into the boundary condition at the wall. Figure 7 displays the solution of the generalized Poisson-Fermi equation solved self-consistently with the Bruggeman model for ions in water. Even though the charge density of the wall is rather moderate, we can observe a significant change of the effective dielectric constant across the solution, which translates into a discrepancy with the model of homogeneous medium. The volume fraction of counterions near the wall becomes higher than in a homogeneous medium because the effective dielectric constant is locally reduced. Such an adsorption was reported in electrostatic calculations of B-DNA in presence of NaCl and $CaCl_2$ [56]: cations, and especially divalent ones, are strongly adsorbed on the phosphate groups of DNA as a result of the dielectric effects arising from the ion packing.

The effective dielectric constant $\varepsilon_{\mathrm{eff}}$ should also include two additional effects due to the dynamic of the water structure around the ions, namely, (i) the kinetic depolarization and (ii) the structure saturation. These effects can yield a small dielectric decrement with respect to the Bruggeman model as reported experimentally for aqueous NaCl solutions at various concentrations [57].

IV. CONCLUSION

We have established a generalized Poisson-Fermi formalism to compute the electrostatic potential in the presence of multiple polydisperse ions. The theory provides insight into size correlation effects such as the depletion of ions at decreasing valences which gives rise to their hierarchical stratification. We have also proposed to address the variations of effective dielectric constant by using self-consistently the Bruggeman model (25).

In a future work, the domain of validity of the generalized Fermi-like distribution (19) will be investigated in terms of dispersion of excluded volumes. In particular, the refined version presented in the Appendix will be evaluated and the role of the effective excluded volume ϑ identified. Monte Carlo simulations and density functional theory may be valuable for comparison as they can help assess the error lying within the higher-order terms in the expansion of the excess free energy. It should be noted that in order to accurately and quantitatively incorporate correlation effects, a nonlocal theory is needed, for example, by including convolutions of the ion direct correlation function with ionic density. A local theory as presented herein can only be justified if the system shows inhomogeneities on length scales that are larger than the typical correlation length. Such a nonlocal approximation in density functional theory for particles of any shape has yet to be worked out, and meanwhile, the generalized Poisson-Fermi formalism offers a compromise between accuracy and computational cost.

We believe that the generalized Poisson-Fermi formalism can reveal a number of other theoretical features regarding the ion size effects. The generalized Fermi-like distribution (19) can be implemented into existing nonlinear Poisson-Boltzmann solvers such as DELPHI [4] or the Adaptive Poisson-Boltzmann Solver (APBS) software package [58], and applied to realistic macromolecular geometries. The existing numerical models of biomolecules can be reused without specific modification. The methodology can be employed to assess the binding properties of large ions to lipid membranes by electrophoretic mobility [12,13]. The experimental mobilities could be compared to numerical values obtained by solving the electrokinetic equations [1] consistently with the generalized Poisson-Fermi formalism along with a Langmuir adsorption model to account for the binding mechanisms at the surface of the membrane. The ion atmosphere around a complex biomolecule such as DNA given by our theory can be also confronted to experimental data obtained by buffer equilibration and atomic emission spectroscopy [59]. Indeed, this technique emphasized the ion size effects on the association of large ions to DNA which cannot be described by the classical Poisson-Boltzmann theory.

ACKNOWLEDGMENTS

I have benefited from fruitful discussions with Alberto Martín-Molina and Manuel Quesada-Pérez. This work was funded by the Agency for Science, Technology and Research (A*STAR) in Singapore.

APPENDIX

The generalized Fermi-like distribution (19) can be refined by taking into account higher-order terms in the expansion of the chemical potential. The idea is to assume that the functionals ΔS_i appearing in the expansion (11) are small compared to the first term. This is because they are made of the difference of functions that are expected to be close to each other. If we approximate the chemical potentials by retaining the terms in $\varepsilon_{v,i}$ but dropping out those in $\varepsilon_{v,i}\Delta S_i$, we end up with

$$\mu_i(\beta,\psi,c_1,\ldots,c_M;v_1,\ldots,v_M) \approx z_i e\psi + k_B T \ln(c_i\Lambda_i^3) - k_B T\frac{v_i}{\vartheta}\ln\phi_{\mathrm{FS}} + k_B T\left(1-\frac{v_i}{\vartheta}\right). \tag{A1}$$

After expressing the thermodynamic equilibrium for the chemical potentials of each ion species, and recombining the equations so as to have only the volume fraction of species i as a function of the electrostatic potential, we obtain the following nonlinear relation:

$$\left\{\phi_{\mathrm{FS}}^{\infty}+\sum_{j=1}^{M}\exp(-z_j\psi^*)\phi_j^{\infty}\left[\left(\exp(z_i\psi^*)\frac{\phi_i}{\phi_i^{\infty}}\right)^{1/1+\delta_i}\right]^{\delta_j}\right\} \times\left(\exp(z_i\psi^*)\frac{\phi_i}{\phi_i^{\infty}}\right)^{1/1+\delta_i}=1, \tag{A2}$$

with $1+\delta_i \equiv v_i/\vartheta$. This equation cannot be solved analytically in the general case. A numerical solution can be obtained by employing an iterative method starting with the generalized Fermi-like distribution (19). In addition, perturbation theory can provide an expansion of the solution which may offer more insight into the physics behind, with a loss of accuracy though. Accordingly, we assume that the solution takes the form

$$\phi_i = \phi_{i,0}\left(1+\sum_{j=1}^{M}\phi_{ij,1}\delta_j + o(\max_j|\delta_j|)\right). \tag{A3}$$

After injection into the nonlinear relation (A2) and identification of the polynomial multipliers, we obtain

$$\phi_{i,0} = \frac{1}{\Phi}\exp(-z_i\psi^*)\phi_i^{\infty},$$

$$\phi_{ij,1} = \frac{\ln\Phi}{\Phi}\exp(-z_j\psi^*)\phi_j^{\infty},$$

$$\phi_{ii,1} = \ln\Phi\left(\frac{1}{\Phi}\exp(-z_i\psi^*)\phi_i^{\infty}-1\right) \tag{A4}$$

with $\Phi=\phi_{\mathrm{FS}}^{\infty}+\Sigma_{k=1}^{M}\exp(-z_k\Psi^*)\phi_k^{\infty}$.

Expectedly, we recover the generalized Fermi-like distribution (19) in the first term of the expansion.

The effective excluded volume ϑ has been so far left aside because it does not appear in the generalized Fermi-like distribution (19). However, in order to compute the free energy (21) or to employ the nonlinear relation (A2) to cal-

culate the ionic volume fractions, we need an analytical expression. In addition to the constraints formulated in (10), we can intuitively understand that the entropy of free space S_{FS} must conserve a symmetric form when an ion species i is either of negligible size $[\forall \mathbf{r} v_i(\mathbf{r})=0]$ or in a vanishing concentration $[\forall \mathbf{r} c_i(\mathbf{r})=0]$. In short, this reads

$$\left.\begin{aligned} &S_{\mathrm{FS}}(c_1,\ldots,c_i=0,\ldots,c_M;v_1,\ldots,v_M)\\ &S_{\mathrm{FS}}(c_1,\ldots,c_M;v_1,\ldots,v_i=0,\ldots,v_M)\end{aligned}\right\}$$
$$= S_{\mathrm{FS}}(c_1,\ldots,c_{i-1},c_{i+1},\ldots,c_M;v_1,\ldots,v_{i-1},v_{i+1},\ldots,v_M). \tag{A5}$$

Especially, the first term in expansion (11) must follow this condition. This is inherently true for the volume fraction of free space ϕ_{FS}, and it must therefore be forced for the effective excluded volume ϑ which we can make depend upon the bulk concentrations. An expression of practical interest would be therefore the mean excluded volume averaged by the volume fractions in the bulk, i.e.,

$$\vartheta(v_1,\ldots,v_M)=\frac{\sum_{i=1}^{M}\phi_i^{\infty}v_i}{\sum_{i=1}^{M}\phi_i^{\infty}}. \tag{A6}$$

[1] R. J. Hunter, *Foundations of Colloid Science* (Oxford University Press, New York, 2001).
[2] D. Andelman, in *Soft Condensed Matter Physics in Molecular and Cell Biology*, edited by W. C. K. Poon and D. Andelman (Taylor and Francis Group, Boca Raton, 2006).
[3] C. F. Wong and J. A. McCammon, Annu. Rev. Pharmacol. Toxicol. **43**, 31 (2003).
[4] W. Rocchia, E. Alexov, and B. Honig, J. Phys. Chem. B **105**, 6507 (2001).
[5] B. Honig and A. Nicholls, Science **268**, 1144 (1995).
[6] B. A. Todd *et al.*, Biophys. J. **94**, 4775 (2008).
[7] A. Savelyev and G. A. Papoian, J. Am. Chem. Soc. **129**, 6060 (2007).
[8] E. Raspaud, D. Durand, and F. Livolant, Biophys. J. **88**, 392 (2005).
[9] P. Hsiao, J. Phys. Chem. B **112**, 7347 (2008).
[10] W. M. Gelbart *et al.*, Phys. Today **53**, 38 (2000).
[11] V. A. Bloomfield, Biopolymers **44**, 269 (1997).
[12] S. A. Tatulian, in *Surface Chemistry and Electrochemistry of Membranes*, edited by T. S. Sørensen (Marcel Dekker, New York, 1999), p. 872.
[13] S. A. Tatulian, J. Phys. Chem. **98**, 4963 (1994).
[14] A. McLaughlin, C. Grathwohl, and S. McLaughlin, Biochim. Biophys. Acta **513**, 338 (1978).
[15] G. Tresset, W. C. D. Cheong, and Y. M. Lam, J. Phys. Chem. B **111**, 14233 (2007).
[16] G. Tresset *et al.*, Biophys. J. **93**, 637 (2007).
[17] C. R. Safinya, Curr. Opin. Struct. Biol. **11**, 440 (2001).
[18] W. M. Gelbart and A. Ben-Shaul, J. Phys. Chem. **100**, 13169 (1996).
[19] V. K. Misra and D. E. Draper, J. Mol. Biol. **299**, 813 (2000).
[20] V. K. Misra and D. E. Draper, J. Mol. Biol. **294**, 1135 (1999).
[21] K. Giewekemeyer, and T. Salditt, Europhys. Lett. **79**, 18003 (2007).
[22] V. Vlachy, Annu. Rev. Phys. Chem. **50**, 145 (1999).
[23] J. P. Hansen, and I. R. McDonald, *Theory of Simple Liquids* (Academic Press, Amsterdam, 2006).
[24] H. L. Vörtler, K. Schäfer, and W. R. Smith, J. Phys. Chem. B **112**, 4656 (2008).
[25] M. Quesada-Pérez *et al.*, Colloids Surf., A **267**, 24 (2005).
[26] M. Quesada-Pérez, A. Martin-Molina, and R. Hidalgo-Alvarez, J. Chem. Phys. **121**, 8618 (2004).
[27] A. Martín-Molina *et al.*, Colloids Surf., A **222**, 155 (2003).
[28] A. Y. Grosberg, T. T. Nguyen, and B. I. Shklovskii, Rev. Mod. Phys. **74**, 329 (2002).
[29] J. Forsman, Langmuir **23**, 5515 (2007).
[30] J. Forsman, J. Phys. Chem. B **108**, 9236 (2004).
[31] B. I. Shklovskii, Phys. Rev. E **60**, 5802 (1999).
[32] Y. Levin, Rep. Prog. Phys. **65**, 1577 (2002).
[33] H. Greberg and R. Kjellander, J. Chem. Phys. **108**, 2940 (1998).
[34] F. Jiménez-Ángeles and M. Lozada-Cassou, J. Phys. Chem. B **108**, 7286 (2004).
[35] A. Tulpar, P. R. Van Tassel, and J. Y. Walz, Langmuir **22**, 2876 (2006).
[36] G. Luo *et al.*, Science **311**, 216 (2006).
[37] A. A. Kornyshev, J. Phys. Chem. B **111**, 5545 (2007).
[38] Y. Chen and J. D. Weeks, Proc. Natl. Acad. Sci. U.S.A. **103**, 7560 (2006).
[39] J. Che *et al.*, J. Phys. Chem. B **112**, 3058 (2008).
[40] J. M. Pimbley, Am. J. Phys. **54**, 54 (1986).
[41] P. de Gennes, *Scaling Concepts in Polymer Physics* (Cornell University Press, Ithaca, 1979).
[42] D. Frenkel and A. Louis, Phys. Rev. Lett. **68**, 3363 (1992).
[43] V. Kralj-Iglič and A. Iglič, J. Phys. II **6**, 477 (1996).
[44] M. Eigen, and E. Wicke, J. Phys. Chem. **58**, 702 (1954).
[45] I. Borukhov, D. Andelman, and H. Orland, Phys. Rev. Lett. **79**, 435 (1997).
[46] Y. Yu, J. Wu, and G. Gao, J. Chem. Phys. **120**, 7223 (2004).
[47] Y. Yu and J. Wu, J. Chem. Phys. **117**, 10156 (2002).
[48] J. Wu and Z. Li, Annu. Rev. Phys. Chem. **58**, 85 (2007).
[49] J. Wu, AIChE J. **52**, 1169 (2006).
[50] D. Gillespie, W. Nonner, and R. S. Eisenberg, Phys. Rev. E **68**, 031503 (2003).
[51] D. Antypov, M. C. Barbosa, and C. Holm, Phys. Rev. E **71**, 061106 (2005).
[52] V. B. Chu *et al.*, Biophys. J. **93**, 3202 (2007).
[53] D. Chandler, *Introduction to Modern Statistical Mechanics* (Oxford University Press, New York, 1987).
[54] F. Henry and L. C. Costa, Physica B **387**, 250 (2007).
[55] D. A. G. Bruggeman, Ann. Phys. **24**, 636 (1935).
[56] S. Gavryushov, J. Phys. Chem. B **112**, 8955 (2008).
[57] K. Nörtemann, J. Hilland, and U. Kaatze, J. Phys. Chem. A **101**, 6864 (1997).
[58] N. A. Baker *et al.*, Proc. Natl. Acad. Sci. U.S.A. **98**, 10037 (2001).
[59] Y. Bai *et al.*, J. Am. Chem. Soc. **129**, 14981 (2007).